,

Quantum Annealing for Air Traffic Management

Tobias Stollenwerk
German Aerospace Center, Linder Höhe, 51147 Cologne, Germany

Bryan O'Gorman, Salvatore Mandrà, and Eleanor G. Rieffel
NASA Ames, Moffet Blvd, Mountain View, CA 94035, USA
(Dated: May 15, 2017)

CONTENTS

LIST OF FIGURES

I. INTRODUCTION

Efficiently automating air traffic management is increasingly important (increased volume and diversity, environmental concerns, etc.).

Quantum annealing is a promising computational method.

We investigate the feasability of applying quantum annealing to a particular problem in air traffic management known as "deconflicting", in which the goal is to modify a set of independently optimal trajectories in a way that removes conflicts between them while minimizing the cost of doing so.

II. PROBLEM SPECIFICATION

Formally, an instance of the deconflicting problem is a set of ideal trajectories

The problem at hand is the deconflicting of transatlantic wind-optimal trajectories. As it was done in [1] we are using the same wind-optimal trajectories of a single day, July 29 2012. These wind-optimal trajectories are given as $(\mathbf{x}_i)_{i=1}^{n}$, where $\mathbf{x}_i = (x_{i,t})_{t=t_{i,0}}^{t_{i,1}}$ and $x_{i,t}$ is the location (as latitude, longitude, and altitude) of the ith flight at time t. The times $t_{i,0}$ and $t_{i,1}$ are the times at which the wind-optimal trajectory for the ith flight begins and ends, respectively. Furthermore, the times are

given in units of one minutes $T_i = (t_{i,0}, t_{i,0}+1, \ldots, t_{i,1})$. Each flight i is at a constant speed v_i, to within (classical) machine precision.

A conflict between two flights is defined as a pair of trajectory points which are too close to each other in space and time.

$$\{(x_{i,t}, x_{j,t'}) \mid \mathcal{D}(x_{i,t}, x_{j,t'}) < \Delta_x, |t-t'| < \Delta_t\} \ , \quad (1)$$

where $\mathcal{D}(x,y)$ is the spatial distance between two points x and y given as latitude, longitude and altitude. Following [1], the space threshold is $\Delta_x = 3$ nautical miles and the time threshold is $\Delta_t = 3$ minutes. In this paper, we consider the following means to deconflict the trajectories: First, we can delay each flight i at departure time by a departure delay d_i

$$x_{i,t} \to x_{i,t+d_i} \quad \forall\, t \in T_i$$

Second, we can avoid a conflict by maneuvers of both involved flights. We assume, however, that the maneuvers will not introduce new conflicts. In doing so, these maneuvers can be view as resulting in time shifts only.

A. Potential Conflicts

It is beneficial to reduce the data to conflicting regions in space and decoupling the spacial and temporal components of the problem. As a first step, we detect all pairs of trajectory points which are separated by a spacial distance below Δ_x

$$\{(x_{i,t}, x_{j,t'}) \mid \mathcal{D}(x_{i,t}, x_{j,t'}) < \Delta_x\} \ ,$$

Two spatially conflicting trajectory points might never become conflicting in time if the corresponding times are far apart. By introducing a constant maximum delay D_{max} we can dismiss all spatial conflicts which can never become conflicting in time

$$\{(x_{i,t}, x_{j,t'}) \mid \mathcal{D}(x_{i,t}, x_{j,t'}) < \Delta_x, |t-t'| \geq \Delta_t + D_{\max}\} \ .$$

With this, we are left with a set of potentially conflicting pairs of trajectory points

$$C_0^{ij} = \{(x_{i,t}, x_{j,t'}) \mid \mathcal{D}(x_{i,t}, x_{j,t'}) < \Delta_x, |t-t'| < \Delta_t + D_{\max}\} \ .$$

As a next step, we group together conflicting trajectory point pairs which are subsequent in time

$$\begin{aligned} C_{\parallel}^{ij} = \{((x_{i,t}, x_{j,t'}), (x_{i,s}, x_{j,s'})) \mid\ & (x_{i,t}, x_{j,t'}) \in C_0^{ij}, \\ & (x_{i,s}, x_{j,s'}) \in C_0^{ij}, \\ & |t-s| < \Delta_t', \\ & |t'-s'| < \Delta_t'\} \end{aligned}$$

where we set $\Delta_t' = 2$ minutes.

For a given pair of flights (i,j) there might be multiple "disjoint" subsets in $C_{\parallel}^{ij}$

$$\bigcup_n C_{\parallel n}^{ij} = C_{\parallel}^{ij}$$

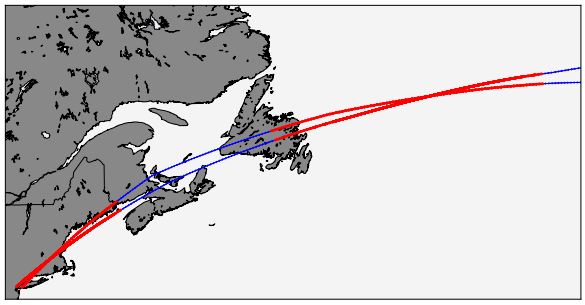

FIG. 1. Example of two parallel potential conflicts between two transatlantic flights starting from the east cost of the USA.

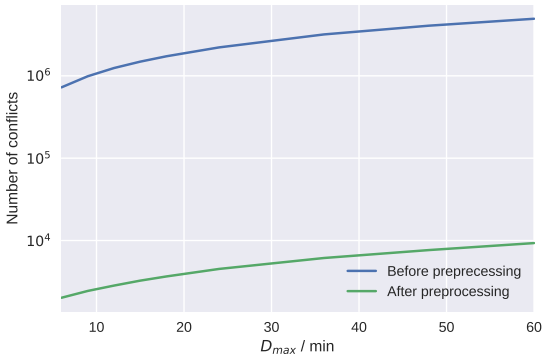

FIG. 2. Preprocessing: Reduction in the number of potential conflicts for various upper delay bounds $D_{\max}$.

where

$$\begin{aligned} & |t-s| \geq \Delta_t' \wedge |t'-s'| \geq \Delta_t' \\ & \forall (x_{i,t}, x_{j,t'}) \in C_{\parallel n}^{ij}, \\ & \forall (x_{i,s}, x_{j,s'}) \in C_{\parallel n'}^{ij}, \\ & n \neq n' \ . \end{aligned}$$

In figure 1 an example of two separated clusters are shown. Together with the remaining, spatially isolated, conflicting trajectory points

$$C_{\times}^{ij} = C_0^{ij} \setminus C_{\parallel}^{ij} \ ,$$

these subsets of trajectory point clusters are called *potential conflicts*.

$$C_k \in C = \{C_{\parallel n}^{ij} | \forall i,j,n\} \cup \{C_{\times}^{ij} | \forall i,j\}$$

Here, we introduced a conflict index $k \in \{1, \ldots, N_c\}$, with $N_c = |C|$. For each conflict index k, we will denote the pair of involved flights by $I_k = (i_k, j_k)$.

Before the preprocessing, the number of conflicts was given by $N_c^{\text{before}} = \sum_{ij} |C_0^{ij}|$. As one can see in figure 2 the preprocessing reduces the number of conflicts by orders of magnitude.

B. Conflict Avoidance

In order to avoid conflicts, a flight i can be either delayed at departure time by d_i or by maneuver introduced delays d_{ik} for each conflict k the flight is involved in. With this, the trajectory times of flight i are shifted

$$\begin{aligned} t &\to t + D_i(t) \ , \\ D_i(t) &= d_i + \sum_{k \in K_i(t)} d_{ik} \ , \end{aligned} \tag{2}$$

where $D_i(t)$ is the delay of flight i at time t and the sum runs over all the conflicts which are before t

$$K_i(t) = \{k \mid \exists x_{i,t'} \in C_k \text{ for which } t' < t\} \ .$$

We introduce the pairs of times of spatially conflicting points inside a conflict k:

$$T_k = \{(t, t') \mid (x_{i,t}, x_{j,t'}) \in C_k, (i,j) \in I_k\} \ .$$

A conflicts k between two flights i and j occurs if the delays are chosen such that a temporal difference between spatially conflicting points is below Δ_t:

$$\begin{aligned} &|t + D_i(t) - t' - D_j(t')| < \Delta_t \\ \Rightarrow &-\Delta_t - (t - t') < D_i(t) - D_j(t') < \Delta_t - (t - t') \ , \end{aligned}$$

for any $(t, t') \in T_k$. Hence a conflict k is avoided if

$$D_i(t) - D_j(t') \notin D_k \qquad \forall\, (t, t') \in T_k \ .$$

with

$$D_k = \left(-\Delta_t - \max_{(t,t') \in T_k} (t - t'), \Delta_t - \min_{(t,t') \in T_k} (t - t') \right) \ .$$

C. Instances

To investigate the problem we consider each flight as a vertex of a graph and each conflict between two flights as an edge of this graph. The connected components of this *conflict graph* represent natural subsets of the problem.

III. CONFIGURATION SPACE RESTRICTIONS

It is important to understand how the restrictions to the configuration space by (4) influence the solution quality. Therefore we solve (3) with a constraint programming solver [2] for various delay discretizations and upper bounds as well as for the continuous problem. As problem instances we used most of the connected components of the conflict graph for $D_{\max} = 18$ minutes with up to $N_f = 50$ flights and $N_c = 104$ conflicts.

In figure 3 one can see the results for a problem instance extracted from a connected component of the conflict graph with $N_f = 19$ flights and $N_c = 47$ conflicts.

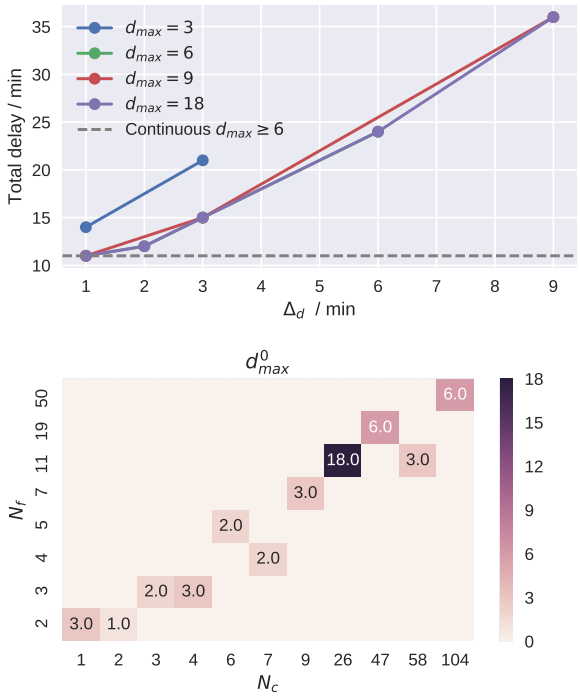

FIG. 3. Top: Total delay of constraint programming solutions for a problem instance with $N_f = 19$ flights and $N_c = 47$ conflicts for various discretization parameters. Bottom: Minimum $d_{\max}$ which yield optimal solution in continuous problem for various problem instances. For all problem instances we used $D_{\max} = 18$ minutes.

With the exception of the small maximum delay $d_{\max} = 3$ min, the total delay of the solutions is nearly independent of the maximum delay. Moreover it is monotonically increasing with the coarseness of the discretization. Since the original data is discretized in time in units of 1 minute, $\Delta_t = 1$ yield the same result as a continuous variable with the same upper bound. Obviously the total delay for the continuous solution decreases monotonically with $d_{\max}$. Above a certain value $d^0_{\max}$ the total delay stays the same. With one exception, we found that for all the investigated problem instances $d^0_{\max} \leq 6$ minutes (see figure 3). Therefore we conclude, that a moderate maximum delay is sufficient even for larger problem instances. On the other hand, the delay discretization should be as fine as possible to obtain a high quality solutions.

IV. MAPPING TO QUBO

A. Departure delays

In this section we describe a simplified version of the above problem. We restrict ourselves to departure delays and neglect maneuvers. Hence the optimization problem

can be written as

$$\min_{d_i} \sum_i d_i$$
$$\text{s.t.} \quad d_i - d_j \notin D_k \qquad \forall\,(t,t') \in T_k \tag{3}$$

The problem needs to be mapped to a quadratic binary optimization problem (QUBO) in order to be solvable by a D-Wave quantum annealer. As a first step, we introduce a discretization and upper bound for the departure delay variables

$$d_i \in \{0, \Delta_d, 2\Delta_d, \ldots, d_{\max}\}\,,$$

where $d_{\max} = N_d \Delta_d$ and $(N_d + 1)$ is the number of delay steps. With this we can write the departure delay variables in terms of new binary variables $d_{i\alpha}$ by

$$d_i = \sum_\alpha \alpha d_{i\alpha}$$
$$\alpha \in \{0, \Delta_d, 2\Delta_d, \ldots, d_{\max}\}\,. \tag{4}$$

However, this approach requires $\sum_\alpha d_{i\alpha} = 1$ to have a unique representation of d_i by $d_{i\alpha}$. This is achieved by adding the following contribution to the QUBO

$$Q_{\text{unique}} = \lambda_{\text{unique}} \sum_i \left(\sum_\alpha d_{i\alpha} - 1 \right)^2 . \tag{5}$$

where λ_{unique} is a penalty weight sufficiently large to ensure $Q_{\text{unique}} = 0$ for the solution. The cost function in (3) yields contribution

$$Q_{\text{delay}} = \frac{1}{d_{\max}} \sum_{i\alpha} \alpha d_{i\alpha}\ , \tag{6}$$

where we have chosen the prefactor $1/d_{\max}$ for convenience. The last contribution to the QUBO represents the conflict avoidance

$$Q_{\text{conflict}} = \lambda_{\text{conflict}} \sum_k \sum_{(\alpha,\beta)\in A_k} d_{i\alpha} d_{j\alpha} \Big|_{i,j\in I_k} \tag{7}$$

where A_k is the set of all (α, β) which correspond to a conflict

$$A_k = \{(\alpha,\beta) \mid \alpha - \beta \in D_k\}$$

Again, $\lambda_{\text{conflict}}$ is the penalty weight for this contribution which have to be chosen large enough to ensure $Q_{\text{conflict}} = 0$ for the solution. The total QUBO of the departure delay model then reads

$$Q_{\text{DDM}} = Q_{\text{delay}} + Q_{\text{unique}} + Q_{\text{conflict}}$$

B. Maneuvers

A more realistic model of the problem can be created by including maneuvers. As mentioned above the maneuvers enter our formulation as additional delays d_{ik} at the conflict time. In the course of mapping to a QUBO formulation, we need to make sure to retain the combinatorial nature of the problem. We do this by restricting the vast realm of maneuvers to two distinct choices: Only one of the two involved flights is delayed while leaving the other flight untouched

$$\text{if } d_{ik} \neq 0 \Rightarrow d_{jk} = 0 \qquad \forall (i,j) \in I_k\ \forall k\ . \tag{8}$$

Moreover, we set the resulting maneuver delays to a constant value d_M large enough to capture all kinds of real maneuvers. A natural choice for this is the temporal conflict threshold $d_M = \Delta_t$.

With (2) we can introduce the delay a flight i at the conflict k as

$$D_{ik} = d_i + \sum_{k'<k} d_{ik}\ , \tag{9}$$

where we have defined a temporal ordering of the conflicts for each flight i by

$$k < p \text{ if } t < t'$$
$$\text{for } t = \arg\min_s x_{i,s} \in C_k\ ,$$
$$t' = \arg\min_s x_{i,s} \in C_p$$

The departure delay variables are represented by binary variables as it was done in section IV A. The maneuver delays are given by

$$d_{ik} = d_M a_{ik} \qquad a_{ik} \in \{0,1\}$$

Since the total delay is given by $\sum_{ik} D_{ik}$, we can write the corresponding QUBO contribution as

$$\tilde{Q}_{\text{delay}} = \sum_{i\alpha} \alpha d_{i\alpha} + \sum_{ik} d_M a_{ik}\ ,$$

For the conflict avoidance, we need to introduce another variable representing the delay at a given conflict

$$D_{ik} = \sum_\delta \delta \Delta_{ik\delta} \qquad \Delta_{ik\delta} \in \{0,1\}\ .$$

By restricting ourselves to $\Delta_d = \Delta_t$ the values of δ in the above equation are given as

$$\delta \in \{0, \Delta_t, 2\Delta_t, \ldots, (N_d + M_{ik})\Delta_t\}\ .$$

Here, M_{ik} is the number of conflicts the flight i is involved in before k. In order to fulfill (9) we add the following contribution to the QUBO

$$\tilde{Q}_\Delta = \lambda_\Delta \sum_{ik} \left(\sum_\alpha \alpha d_{i\alpha} + \sum_{k'<k} d_M a_{ik'} - \sum_\delta \delta \Delta_{ik\delta} \right)^2 \Big|_{i,j\in I_k}$$

For unique representation of the variables we add

$$\tilde{Q}_{\text{unique}} = \lambda_{\text{unique}} \left\{ \sum_i \left(\sum_\alpha d_{i\alpha} - 1 \right)^2 + \sum_{ik} \left(\sum_\delta \Delta_{ik\delta} - 1 \right)^2 \right\}\ .$$

Conflicts are avoided if $D_{ik} - D_{jk} \notin D_k$, $(i,j) \in I_k$. The corresponding QUBO contribution reads

$$\tilde{Q}_{\text{conflict}} = \lambda_{\text{conflict}} \sum_k \sum_{(\delta,\delta') \in B_k} \Delta_{ik\delta} \Delta_{jk\delta'} \Big|_{i,j \in I_k}$$

where B_k is the set of all (δ, δ') which correspond to a conflict

$$B_k = \{(\delta, \delta') \mid \delta - \delta' \in D_k\}$$

The penalty weights λ_Δ, λ_{unique} and $\lambda_{\text{conflict}}$ must be chosen large enough to ensure vanishing contributions from the corresponding QUBO terms for the solution.

Finally, the maneuver decision described by (8) is incorporated by a antiferromagnetic coupling between the two maneuver delay variables

$$\tilde{Q}_{\text{maneuver}} = J \sum_k (s_{ik} s_{jk} + 1)_{i,j \in I_k} \ .$$

with

$$s_{ik} = 2a_{ik} - 1 \in \{-1, 1\}$$

and $J > 0$ has to be chosen large enough. A solution is considered to be valid only if $\tilde{Q}_{\text{maneuver}} = 0$. Hence, the total QUBO for the maneuver model reads

$$Q_{\text{MM}} = \tilde{Q}_{\text{delay}} + \tilde{Q}_\Delta + \tilde{Q}_{\text{unique}} + \tilde{Q}_{\text{conflict}} + \tilde{Q}_{\text{maneuver}}$$

C. Choice of the Penalty Weights

The contributions (5) and (7) to the QUBO for the departure delay model of section IV A are hard constraints. This means a solution to the QUBO is only valid if both (5) and (7) vanish. Therefore, the penalty weights λ_{unique} and $\lambda_{\text{conflict}}$ must be chosen sufficiently large to ensure that the hard constraints are fulfilled for the solution to the problem. On the other hand, large penalty weights lead to large differences between the largest and smallest non-vanishing coefficients in the QUBO. Since the D-Wave quantum annealers have a limited resolution for the specification of the QUBO, this can lead to a misspecification of the problem. [3] Hence, it is desirable to find a sweet spot of the smallest penalty weights which still yield valid solutions.

In order to find these optimal penalty weights, we employed an exact solver [4] to explore the validity of a solution in dependence on the penalty weights. We investigated problem instances with up to $N_f = 7$ flights and $N_c = 9$ conflicts. For all these problem instances we found a box like shape of the boundary between valid and invalid solutions as it is depicted in figure 4.

One can give an upper bound for the sufficiently large penalty weights by the following considerations. A minimal violation of the hard constraints yield an additional contribution to the QUBO cost function of λ_{unique} or

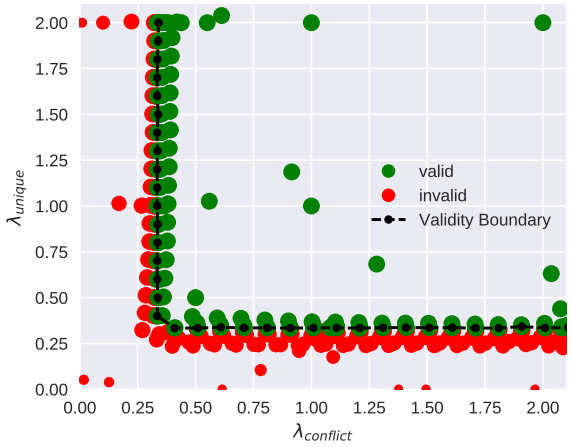

FIG. 4. Validity of exact solution to a QUBO extracted from a problem instance with $N_f = 7$ flights and $N_c = 9$ conflicts in dependence on the choice of the penalty weights, λ_{unique} and $\lambda_{\text{conflict}}$.

$\lambda_{\text{conflict}}$, respectively. As a result of this violation, the contribution from (6) can be reduced maximally by

$$\min_{\{d_{i\alpha}\}} \left\{ \frac{1}{d_{\max}} \sum_{i\alpha} \alpha d_{i\alpha} - \frac{1}{d_{\max}} \sum_{j\beta} \beta d_{j\beta} \right\} = -1$$

Therefore an upper bound for sufficiently large penalty weights is given by

$$\lambda_{\text{unique}} > 1$$
$$\lambda_{\text{conflict}} > 1$$

D. Results from ICM

V. D-WAVE

A. Embedding

B. Quantum Annealing Results

VI. CONCLUSIONS

TODO

VII. ACKNOWLEDGEMENTS

TODO

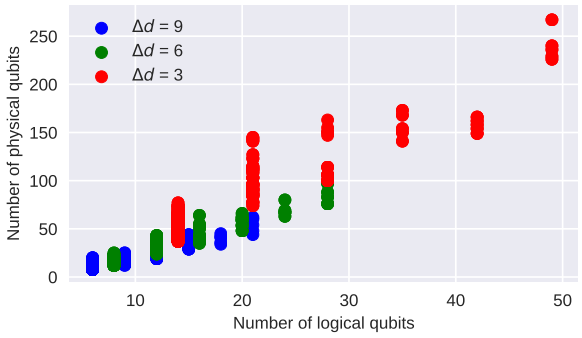

FIG. 5. Number of physical qubits versus the number of logical qubits after embedding of QUBO instances with up to $N_f = 50$ and $N_c = 104$

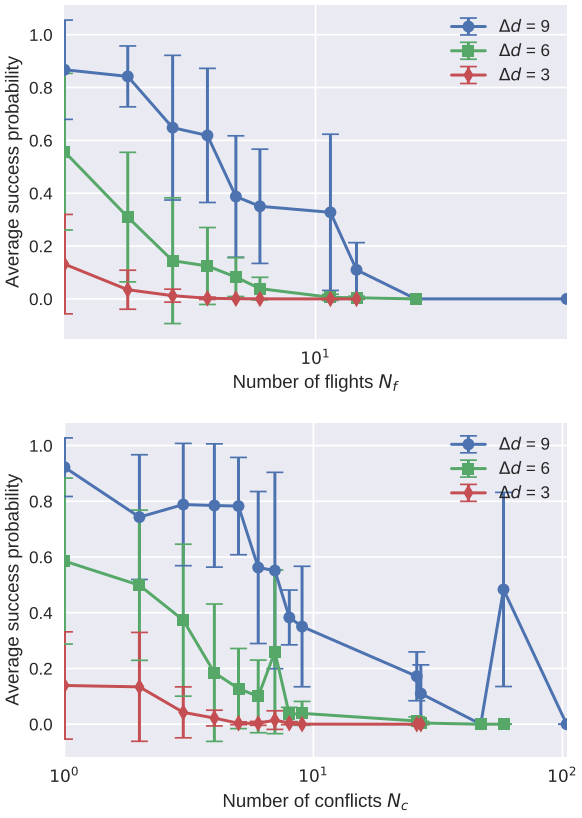

FIG. 6. Success probability for QUBO instances in dependence of the number of flights N_f and the number of conflicts N_c. The error bars indicate the standard deviation. We used 10000 annealing runs for each instance and penalty weights $\lambda = \lambda_{\text{conflict}} = \lambda_{\text{unique}} \in \{0.5, 1, 2\}$.

[1] O. Rodionova, D. Delahaye, B. Sridhar, and H. Ng., Proceedings of Advanced Aircraft Efficiency in a Global Air Transport System (AEGATS'16) Conference (2016).

[2] E. Hebrard, E. O'Mahony, and B. O'Sullivan, "Constraint programming and combinatorial optimisation in numberjack," in *Integration of AI and OR Techniques in*

Constraint Programming for Combinatorial Optimization Problems: 7th International Conference, CPAIOR 2010, Bologna, Italy, June 14-18, 2010. Proceedings, edited by A. Lodi, M. Milano, and P. Toth (Springer Berlin Heidelberg, Berlin, Heidelberg, 2010) pp. 181–185.

[3] Reference to D-Wave limited resolution.

[4] Reference to mapping from QUBO to max sat and to akmaxsat solver.